J. Fluid Mech. (1985), *vol.* 161, *pp.* 217–237
Printed in Great Britain

The effect of sound on vortex shedding from cylinders

By R. D. BLEVINS
GA Technologies Inc., San Diego, California 92138

(Received 2 October 1984 and in revised form 26 April 1985)

The influence of a transverse sound wave on vortex shedding from a rigid circular cylinder in a duct has been explored at Reynolds numbers from 20000 to 40000. In the absence of sound, the vortex shedding is found to consist of strings of coherent cyclic events which have frequencies that wander randomly about the nominal vortex-shedding frequency. Application of sound at the vortex-shedding frequency eliminates this wander and correlates the shedding along the cylinder axis. The frequency of vortex shedding can be shifted by sound applied either above or below the nominal vortex-shedding frequency. This entrainment is produced by the velocity induced by the sound wave rather than by the sound pressure. These phenomena are also observed in tube rows.

1. Introduction

Aeroacoustic sound generated by vortex shedding from cylinders held across a fluid flow has been extensively studied since the experiments by Strouhal in 1878. However, relatively little attention has been paid to the effect of an imposed sound field on vortex shedding. The primary motivation for studying the effect of sound on the fluid mechanics of vortex shedding is to explore the aeroacoustic feedback that occurs when the vortex-induced sound reflects from large stationary surfaces back into the generating cylinder. This reflection and feedback phenomenon is of considerable practical importance. It commonly occurs in tube-and-shell heat exchangers.

Intense sound and vibration in a tube-and-shell heat exchanger can be produced by gas flow across a bank of tubes. Baird (1954) reported intense noise and vibration in the heat exchanger of a power plant above about 90×10^6 Watts power. He measured sound as high as 40 Pa (126 db) outside the heat-exchanger shell and found that the vibration was associated with a standing acoustic wave across the duct containing the heat-exchanger tube bundle. Baird attributed the sound to vortex shedding from the heat-exchanger tubes at sympathetic acoustic natural frequencies of the gas contained by the heat-exchanger ducting. Thus, the phenomenon is an acoustic resonance. The resonant acoustic modes were transverse to both the mean gas flow and the tube axis.

Grotz & Arnold (1956) and Putnam (1965) performed studies of the acoustic resonance of air flow through tube banks in rectangular ducts. The acoustic resonance has been observed in tube banks with tubes on rectangular patterns (i.e. in-line) and triangular patterns (i.e. staggered), tube rows, chemical-process heat exchangers, boilers and power plants (Blevins 1984). Sound levels as high as 6300 Pa (170 db) have been observed in the pressurized CO_2 of nuclear-power-plant steam generators and as high as 3500 Pa (165 db) in air (Baylac & Gregoire 1975; Donaldson & McKnight

1979). These sound levels are sufficient to damage shell structures, and they are hazardous to the hearing of humans.

Okamoto, Hirose & Adachi (1981) examined the effect of an acoustic wave propagating parallel to the cylinder axis on vortex shedding. He found some effect at sound levels above about 20 Pa (120 db). Richardson (1967) reported that ambient sound can increase heat transfer from tubes. This suggests the presence of an acoustic-vortex feedback which increases the turbulent momentum and hence the heat transfer upon application of the acoustic wave. In a study of shear wave instability, Peterka & Richardson (1969) imposed sound on a cylinder in a free jet at frequencies about a factor of 10 above the vortex-shedding frequency. They concluded that sound at these frequencies enhances vortex formation and heat transfer but has little effect on the shedding frequency. No study has been made of the effect of sound imposed transverse to the axis of a cylinder (i.e. acoustic velocity induced normal to the cylinder axis) at frequencies at or near the vortex-shedding frequency.

Numerous studies of flow about mechanically vibrated cylinders (see reviews by Sarpkaya 1979; King 1977; Blevins 1977) have demonstrated that transverse cylinder vibration at the vortex-shedding frequency can (i) increase the strength of the shed vortices, (ii) increase the drag of the cylinder, and (iii) synchronize or 'lock in' with vortex shedding so that the vortex-shedding frequency will remain at the cylinder vibration even if the flow velocity is varied. These effects are indicative of a nonlinear feedback mechanism between vortex shedding and the cylinder motion.

This paper describes experiments performed to explore the effect of sound at and near the vortex-shedding frequency on vortex shedding from cylinders and cylinder rows in an air flow in ducts. In all cases, the cylinder axes were perpendicular to both the mean air flow and the imposed sound wave. This case corresponds to the observed acoustic resonances in tubular heat exchangers. In addition, measurements were made of vortex shedding in the absence of sound and of the influence of free-stream turbulence.

2. Description of experimental apparatus and instrumentation

The test rig is shown in figure 1, and a block diagram of the instrumentation is presented in figure 2. Atmospheric air flows through an entrance and two straightening and turbulence suppression grids into a duct of 45.7 cm × 38.1 cm rectangular cross-section which is maintained for 5.5 m through the approach, test and exit sections. The exit section terminates in a conical transition into 61 cm diameter suction ducting. The test section is fabricated from 2.54 cm thick acrylic sheet. The entrance and exit sections are fabricated from 1.905 cm thick plywood coated with epoxy resin.

Turbulence grids can be installed 48.3 cm forward of the test section. The two grids used in this test programme were fabricated from steel rods mounted in a frame on 2.54 cm centres to form a square mesh. The root-mean-square turbulence produced by these grids is given in table 1. These turbulence levels were measured by a movable probe in the empty test section. The grids also tended to produce a more uniform velocity profile in the test section as shown in figure 3.

Both acoustic (pressure sensing) and fluid-velocity instrumentation was employed. The acoustic sensors consisted of two phase-matched Bruel and Kjar 0.635 cm ($\frac{1}{4}$ in.) condenser microphones placed in drilled access ports flush with the wind-tunnel wall. The fluid-velocity instrumentation consisted primarily of 13 flush-film-anemometer

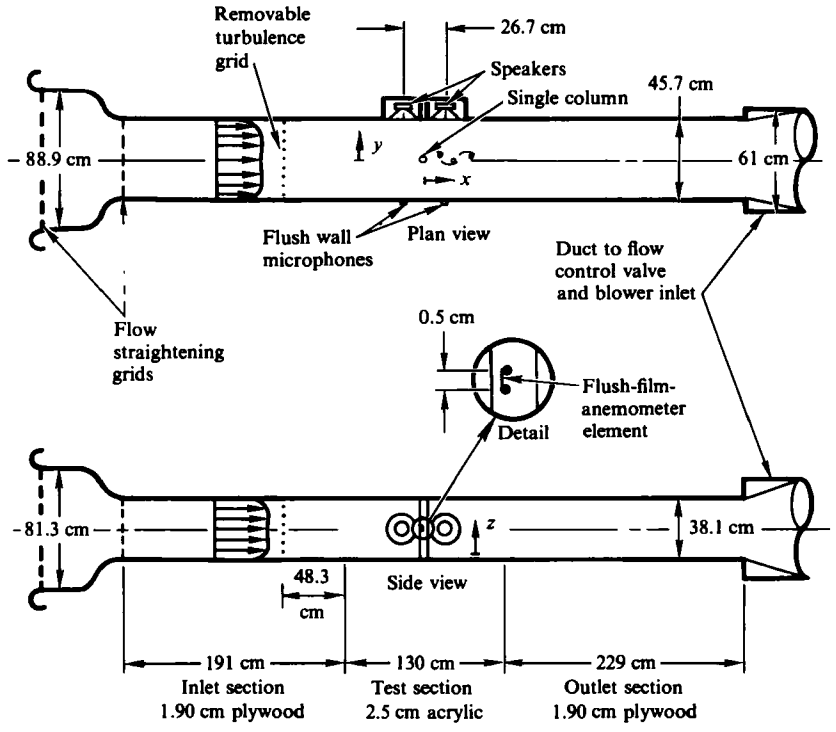

FIGURE 1. Diagrammatic view of wind tunnel.

elements and one cylindrical film-anemometer element mounted in a movable probe. The 1.905 cm outside diameter test cylinder was fabricated from a stainless-steel tube. It was held rigidly at its extremities to the test section. No cylinder vibration was detected during any part of the test programme.

Nine of the flush-film-anemometer elements were located at 3.81 cm intervals along the span of the test cylinder. Their locations are shown in figure 3. The cylinder surface is relieved locally at each gauge and all leads run through the interior of the tube. The element of each flush film is orientated parallel to the tube axis. Care was taken to produce minimal change in the tube contours due to the presence of the gauges. A cylindrical-element anemometer probe was employed along with a conventional Pitot-static tube for measuring mean velocity and turbulence level.

Two electromagnetic speakers are attached to one of the vertical test-section walls along the mid-plane of the wall at equal distances upstream and downstream of the test cylinder. The speakers are driven through an amplifier by a variable-frequency oscillator. They are used to excite a standing acoustic wave in the test section. The rear of the speakers is vented to the interior of the test section to minimize steady loading on the speaker elements. A perforated grid was placed across the mouth of each speaker flush with the inner test-section wall to minimize separation of flow across the speaker mouth.

Data were processed on-line using the two spectral analysers and the strip-chart recorder. The movable-probe signal was calibrated and linearized for computation of turbulence levels. The flush-film anemometers mounted on the test cylinder were not calibrated, and the anemometer output was sent directly to the spectral analysers. Thus, the flush-film anemometers provide only a relative measure of

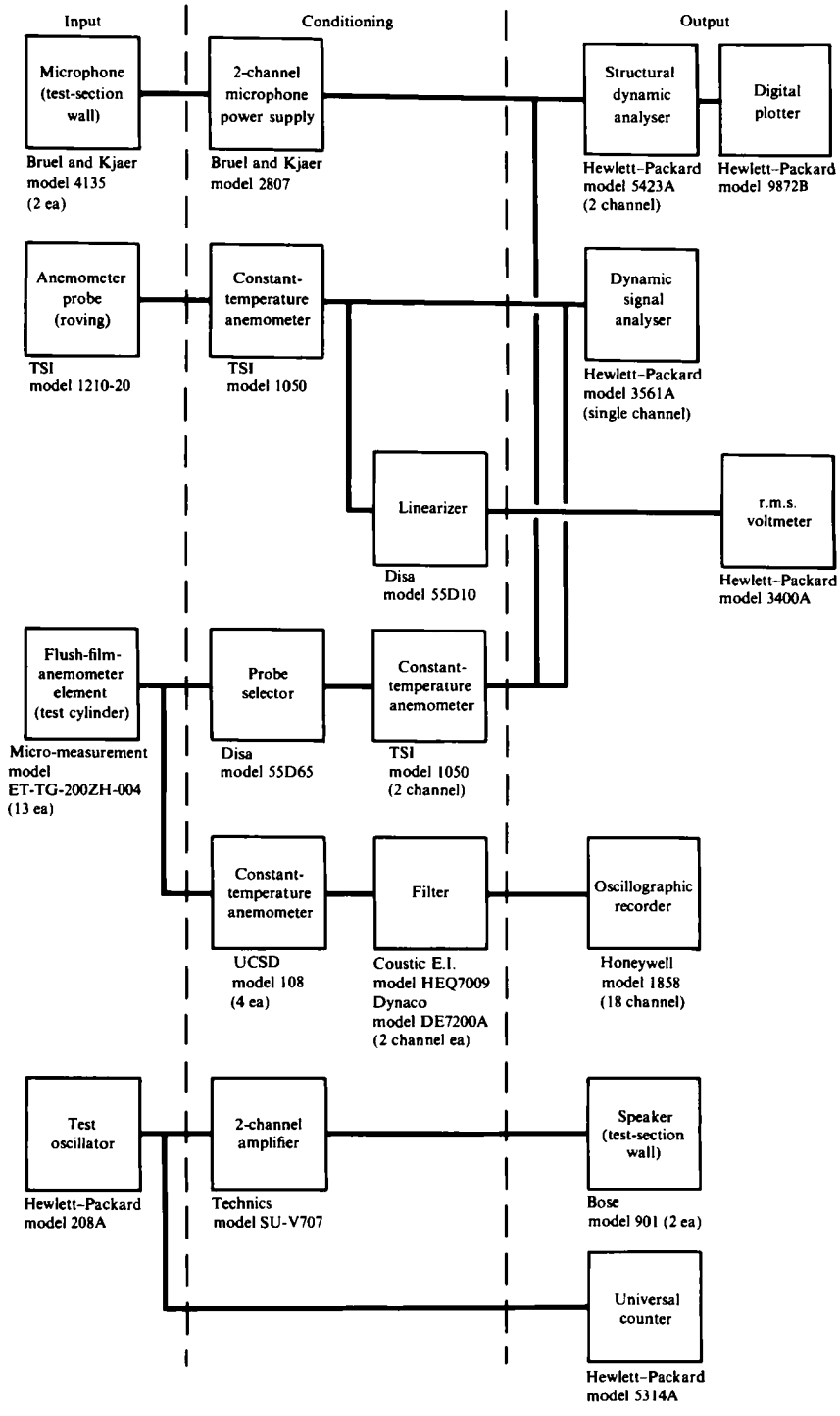

FIGURE 2. Data acquisition and speaker system.

Grid	Centreline velocity 14.6 m/s	29.2 m/s
No grid	0.4	0.8
3.175 mm diameter rods	1.2	1.7
6.35 mm diameter rods	1.8	2.2

TABLE 1. R.m.s. turbulence intensity ($100u'/U$)

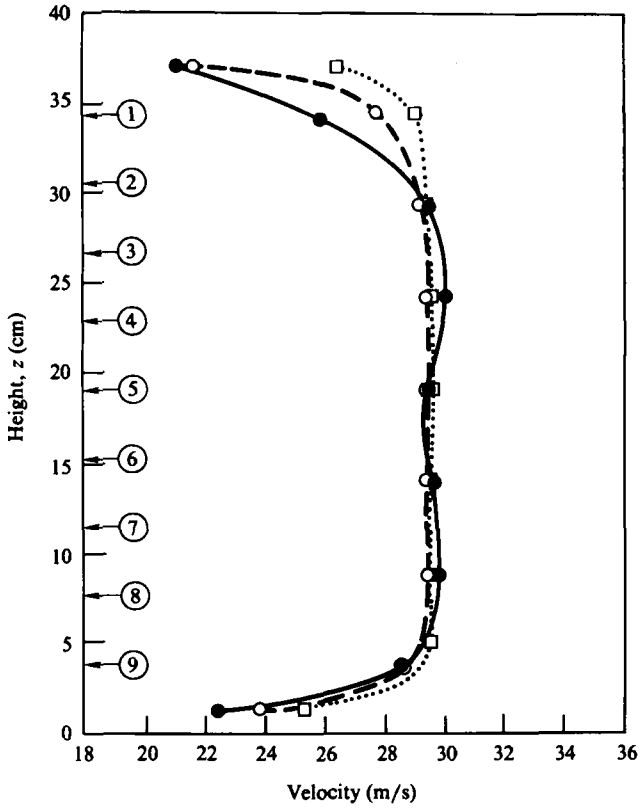

FIGURE 3. Typical velocity profiles at mid-plane of the test section. These velocities were measured with a Pitot-static tube. Circled numbers on left-hand vertical axis give locations of flush-film elements on test cylinder. —●—, no grid; --○--, $\frac{1}{8}$ in. diameter rod grid; ...□..., $\frac{1}{4}$ in. diameter rod grid.

turbulent shear stress on the tube surface. The spectra of the anemometer outputs were typically made over a 50 Hz band centred about the nominal vortex-shedding frequency of 375 Hz corresponding to a flow of 33 m/s. This relatively fine frequency band was used to reveal the details of the vortex-shedding process.

Data taken over a finite time interval are digitized using an A to D converter and processed by an FFT analyser to construct a frequency spectrum. The frequency resolution is a function of the time length of the data-sampling interval. For the present Hewlett–Packard spectral analysers, the number of data points in the

Width (Hz)	Resolution (Hz)	Sampling interval (s)
100	0.390	2.56
50	0.195	5.12
25	0.097	10.24

TABLE 2

sampling interval is fixed, and as a result both the frequency resolution and the length of the sampling interval are a function only of the width of the spectrum (table 2). Thus, 5.12 s of data must be sampled to construct a single spectrum of 50 Hz bandwidth. Average spectra are constructed by continuously averaging spectra from overlapping time samples. These average spectra have no better frequency resolution than the individual spectra, but they more accurately represent the mean properties of the vortex-shedding process.

3. Experiments with a single cylinder without sound

For these experiments, the speakers were not employed, and the single instrumented cylinder was mounted in the centre of the test section. The cylinder was rotated about its axis until the filament of the flush-film-anemometer elements was located 70° aft of the leading edge of the cylinder. This angular orientation produced the greatest signal at the vortex-shedding frequency. It is also the point of boundary-layer separation at Reynolds numbers in the test range. From one to four of the flush films were continuously monitored.

All data reduction was made on-line. For spectral measurements, the output of the flush-film-anemometer elements was sent to the two constant-temperature anemometers and then directly to the one- or two-channel spectral analysers. No intermediate filtering was applied. For time-history records, four channels of University of California, San Diego, anemometers (Itsweire & Hell 1983) were employed (see figures 2 and 3). The resultant signals were filtered to remove frequencies above 500 Hz and at or below 60 Hz to remove line noise, d.c. bias and high-frequency noise inherent in the instrumentation. The resultant time-history signals are relatively clean, and they contain the vast majority of the vortex-shedding response.

When the spectral analysis of the anemometer output was carried out over an extended frequency range with a frequency resolution greater than 3 Hz or multiple spectra were averaged, the spectra showed a single well-defined peak at the vortex-shedding frequency:

$$f_S = S\frac{U}{D}\text{ Hz}, \tag{1}$$

where U is the free-stream velocity, D is the cylinder diameter, and the Strouhal number S is approximately 0.2 in this Reynolds-number range (Roshko 1953). For $U = 33$ m/s, the vortex-shedding peak occurred at about 372 Hz. This peak is shown in figure 4, which is the average of 1000 consecutive spectra made from overlapping time intervals gathered over a continuous period of approximately 13 min. This averaging produces an exceptionally smooth and well-defined spectrum. It has a peak at 372 Hz and bandwidth of about 7 Hz.

In contrast, when the vortex-shedding spectra were examined with a spectral resolution of 1 Hz or finer and only a relatively small number of samples were

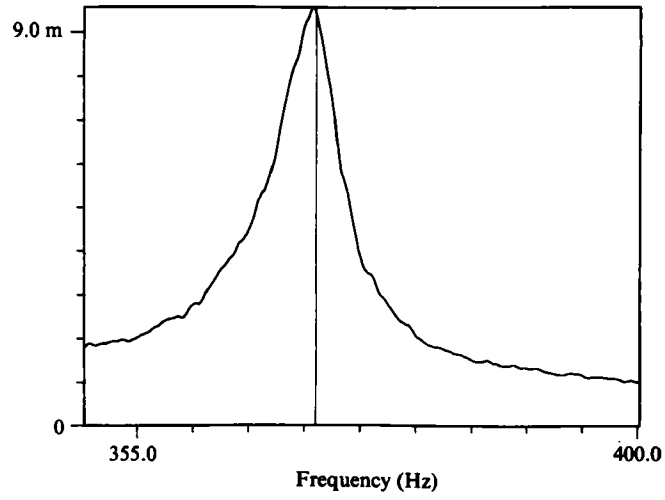

FIGURE 4. Spectrum from flush-film 5 at a centreline velocity of 33.2 m/s. This spectrum is the average of 1000 consecutive spectra made from 5.12 s overlapping time samples.

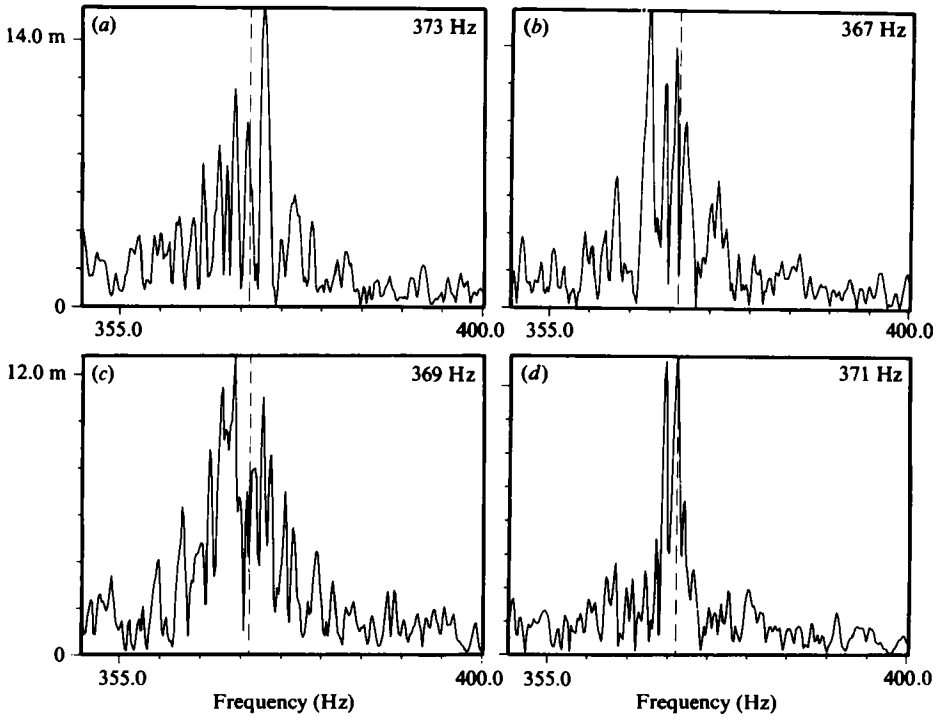

FIGURE 5. Spectra from flush-film 5 at a centreline velocity of 33.2 m/s. Each spectrum represents a single 5.12 s sample. Compare with figure 4.

averaged, a very-different-looking spectrum was obtained, as shown in figure 5. The four spectra were taken at a centreline velocity of 33.2 m/s and a frequency resolution of 0.195 Hz. Each spectrum represents a single 5.12 s sample interval started at randomly chosen times; no spectral averaging or overlap of data was used. Each of the spectra of figure 5 has a unique form and none of them replicate figure 4. The

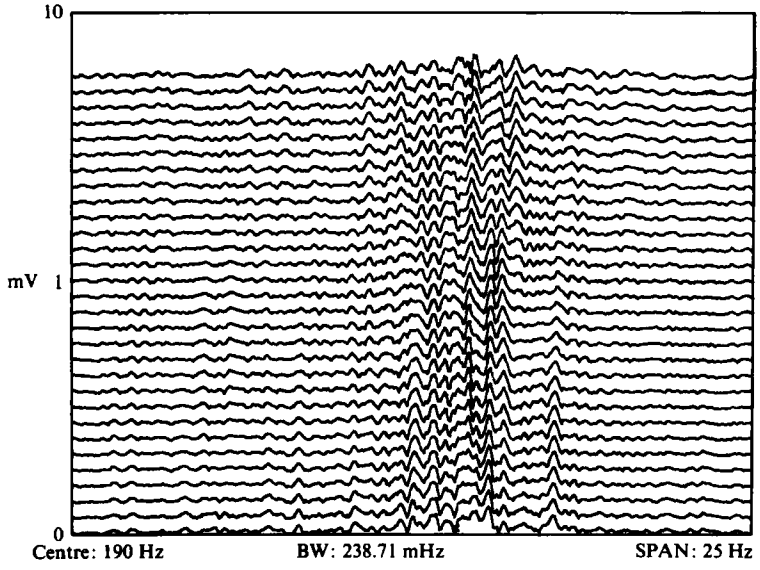

FIGURE 6. Waterfall plot of 30 consecutive spectra taken from flush-film 5 with a centreline mean velocity of 18.3 m/s. Note the variation in the frequency content.

frequency of the highest peak in each spectrum of figure 5 varies from 367 to 373 Hz, and the bandwidth of each of the major peaks is between 1 and 2 Hz. The sharp, narrow-band peaks and the time-to-time variation in the spectra suggest short-duration but well-defined coherent fluid-mechanic structures whose frequencies vary from event to event. It is also easy to see how these events could be averaged over many events to produce the 1000-spectrum average shown in figure 4.

In order to explore this frequency variation more closely, a waterfall plot was constructed of 30 spectra made with overlapping time samples. A typical result is shown in figure 6. The centreline velocity is 18.3 m/s corresponding to a Reynolds number, based on cylinder diameter, of 22800. The time required to construct the first spectrum is 10.24 s, and subsequent spectra utilize substantial portions of the data of the previous spectra. Thus, the rate of evolution of the frequencies shown in figure 6 may be a product of the data processing. However, the fact that the frequencies change with time is inherent in the data.

Finally, to resolve the nature of time variation of vortex shedding, time-history plots of four of the adjacent flush-film outputs were made with a high-speed strip-chart recorder. A typical result is shown in figure 7. While the overall impression of each signal is of a beat produced by two interacting sinusoidal signals, closer examination shows this is not the case. The larger-amplitude pulses are relatively well defined and nearly sinusoidal, whereas in the intermediate ranges of low amplitude, the time histories are often irregular and non-sinusoidal. Other observations on figure 7 are:

(i) The frequency variations are relatively small but distinct (compare the distance between three or four peaks at various points in time).

(ii) There is a tendency for the larger-amplitude pulses to have lower frequency than the lower-amplitude intermediate intervals. These intermediate cycles are often very irregular.

(iii) The signals from the four anemometers are not generally in phase. The phase seems to vary randomly. Adjacent sensors (compare signals 5 and 6 or 7 and 8 with

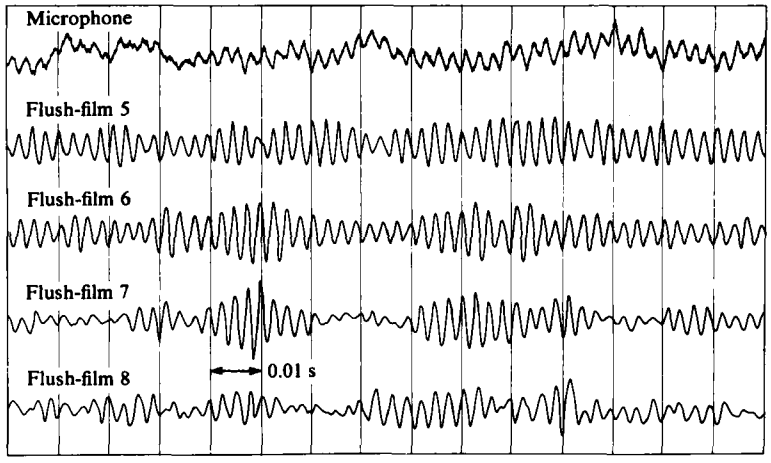

FIGURE 7. Time history of microphone mounted in test-section wall and four flush films along the cylinder span (see figure 3) at $U = 33$ m/s. Note lack of spanwise coherent and irregular cycles. No sound is applied by speakers.

timing marks) are more or less in phase, but widely separated sensors (compare 5 and 8) can be 180° out of phase.

(iv) Similarly, the amplitudes of the four anemometer signals do not vary in unison, but bursts of large amplitude observed on all four sensors do suggest a quasi-two-dimensional overlay, at least for the larger bursts.

In order to eliminate the possibility that the flush-film sensors, their installation details, or the wind tunnel was producing these phenomena, a smooth, uninstrumented cylinder was substituted for the instrumented cylinder and the vortex shedding was monitored with the cylindrical anemometer element on the movable probe. The resultant time histories were substantially the same as shown in figure 7. Thus, it is unlikely that the observed phenomena are a product of the sensors or their installation. Similarly, the fact that the phenomena illustrated in figure 7 do not move in lock step along the span of the cylinder suggests that no pulsation or instability within the wind tunnel was responsible for these phenomena. Moreover, no other 'extraneous' frequency could be found in spectra taken over an extended frequency range, and the same phenomena were observed at all mean velocities tested. Therefore, the author believes that the frequency variation, burst and three-dimensional phenomena previously noted are inherent in the physics of vortex shedding from cylinders in ducts at these Reynolds numbers. It is recognized that these phenomena may be triggered by inlet turbulence or the non-uniformities of the flow profile (figure 3). It remains doubtful if the phenomena would occur in a perfectly uniform profile or without inlet turbulence; they do occur in duct flows over cylinders at these Reynolds numbers.

4. Experiments with sound

As shown in figure 1, the air in the test section can be excited by speakers located in the test-section wall. In the range of frequencies of interest in these tests, the greatest acoustic response (374–388 Hz) occurred at the natural frequency of the fundamental transverse acoustic mode of the test section. The fundamental natural

acoustic frequency did not change appreciably with the presence of a single tube or a single row of tubes, but it did increase from 374 to 380 Hz as ambient air temperature increased from 18 to 25 °C.

Theoretically, the pressure distribution in the rectangular test section at resonance with the first transverse mode is (Morse & Ingard 1968)

$$p = P\cos\left(\frac{\pi y}{L}\right)\cos\omega t. \tag{2}$$

P is the pressure amplitude, y is the transverse coordinate (figure 1), $L = 45.7$ cm is the transverse width, and $\omega = \pi c/L = 2350$ rads/s (375 Hz) is the circular natural frequency of the first transverse mode. The momentum equation,

$$\frac{\partial p}{\partial y} = -\rho\frac{\partial v}{\partial t}, \tag{3}$$

can be used to determine the corresponding transverse acoustic velocity v:

$$\begin{aligned} v &= -\frac{P\pi}{\rho\omega L}\sin\left(\frac{\pi y}{L}\right)\cos\omega t \\ &= \frac{P\pi}{\rho\omega L}\sin\left(\frac{\pi y}{L}\right)\sin(\omega t - \tfrac{1}{2}\pi). \end{aligned} \tag{4}$$

Acoustic velocity lags pressure (2) by 90° in the first mode, and it is maximum at the centre of the test section where acoustic pressure is zero. For atmospheric air, (4) leads to the relationships between the maximum acoustic pressure, which occurs at the walls, and the maximum acoustic velocity, which occurs at mid-section, that are shown in table 3.

The acoustic velocity is generally a small percentage of the mean air velocity and the maximum transverse velocity associated with the fully formed vortices. It is, however, comparable to turbulence r.m.s. velocities.

The acoustic pressure measured in the test section when it is excited at the fundamental mode resonance is compared with theory in figure 8. Neither the fundamental mode nor the acoustic pressure distribution was observed to change with flow or when a single tube or a tube row was placed in the test section. The high degree of agreement between the predicted and measured pressures in the acoustic mode suggests that the acoustic velocity is also accurately predicted by (4).

Excitation of a standing acoustic wave in the test section had a dramatic effect on vortex shedding from a single cylinder in the centre of the test section (figure 1). Figure 9 shows the spectra obtained from the flush films located at the mid-height of the test cylinder with various levels of sound applied at the nominal vortex-shedding frequency. Applied sound reduces the bandwidth of vortex shedding and centres the vortex-shedding frequency at the frequency of the applied sound. These effects increase with the magnitude of the applied sound. (The sound levels reported in figure 9 and the remaining figures in this paper refer to sound pressure measured at the vertical wall opposite the speakers.)

The spectra in figure 9 are the result of 400 consecutively averaged spectra. The averaging accounts for the rounded, relatively smooth appearance of the spectra with no sound (compare with figures 4 and 5). Considering that the single average spectra with no sound are basically narrowband with peaks that wander over about a 6 Hz band (figure 5) and that the velocity induced by sound is a small fraction of the mean velocity, it is reasonable to believe that the sound does not change the nature of the

Pressure amplitude, P		Acoustic velocity amplitude	
Pa	db	v_{acoustic} (m/s)	v_{acoustic}/U (%)
0	0	0	0
60	130	0.145	0.441
120	136	0.291	0.881
250	142	0.606	1.84
500	148	1.212	3.67

$U = 33$ m/s is the typical mean flow velocity in the test section.

TABLE 3

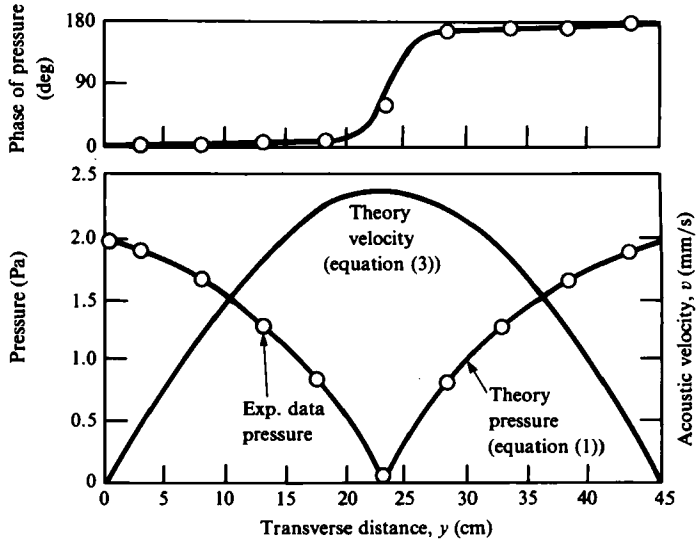

FIGURE 8. Acoustic characteristics of test section when excited at first transverse mode resonance of 374 Hz.

vortex-shedding process but it does synchronize the events at the applied acoustic frequency.

The increase in spanwise correlation of vortex shedding induced by sound can be seen in figure 10. Figure 10 is the corollary to figure 7 with the addition of 300 Pa sound at the shedding frequency of 374 Hz; the gains of films 7 and 8 are also reduced by half from figure 7. Note that all four flush-film signals are nearly in phase with each other and are slightly phase-shifted from the sound at the test-section wall. The amplitude of the film signals is also increased from figure 7. The presence of irregular cycles is diminished (eliminated in the three lower traces), although some beating remains. Thus, the sound has the ability to synchronize the frequency and increase the strength of vortex shedding from cylinders.

Figure 11 shows the phase angle between sound pressure at the test-section wall and flush-film-anemometer element 5 as a function of sound pressure and the frequency shift. In the absence of applied sound, the microphone measures the aeroacoustic sound produced by vortex shedding from the cylinder (see Blevins 1984). As can be seen in figure 7, this sound signal is somewhat irregular but it generally

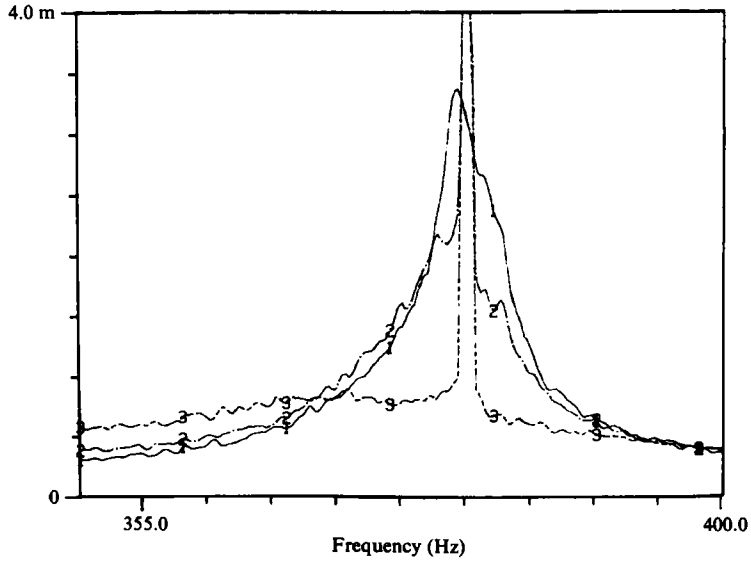

FIGURE 9. Spectra of vortex shedding from flush-film 5 at $U = 36$ m/s and sound applied at the vortex-shedding frequency of 380.5 Hz. This spectrum is the result of 400 consecutively averaged spectra. 1. —, no sound; 2. —·—, 100 Pa; 3. – – – –, 250 Pa. Note the decrease in the bandwidth of vortex shedding as the sound level is increased. The vertical scale is not changed for the three different curves.

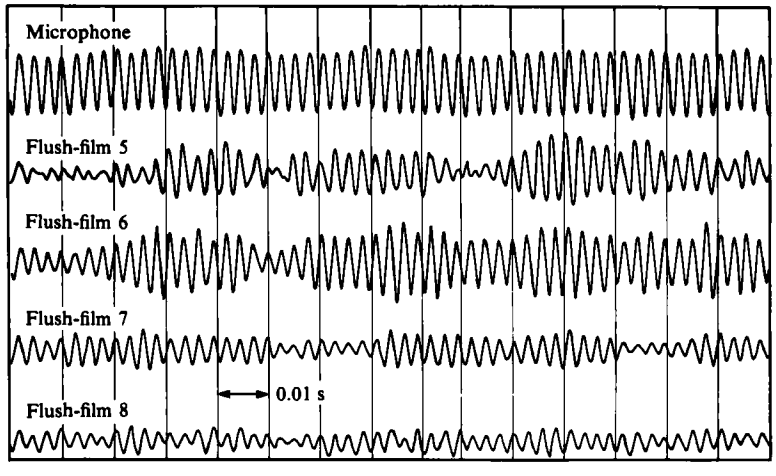

FIGURE 10. Time history of microphone mounted in test-section wall and four flush films (figures 1 and 3) at $U = 33$ m/s. Note high degree of spanwise coherence. 300 Pa sound at 375 Hz is applied by speakers.

leads the flush-film 5 signal by about 90°. When 300 Pa sound is applied at the vortex-shedding frequency (figure 10), this phase angle decreases to about 30°. This downward shift in phase also occurs when sound is applied at frequencies other than the vortex-shedding frequency, but not to the same extent.

Figure 12 shows that the correlation of vortex shedding along the cylinder span increases substantially when sound is applied at the vortex-shedding frequency. This

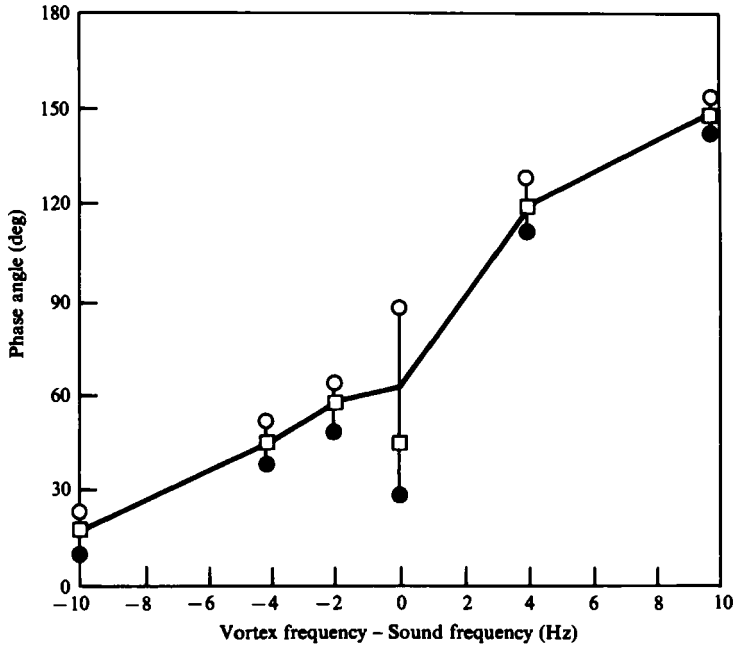

FIGURE 11. Phase angle between sound pressure at test-section wall and centre frequency of vortex shedding. ○, No applied sound. ●, 250 Pa applied sound. □, 100 Pa applied sound.

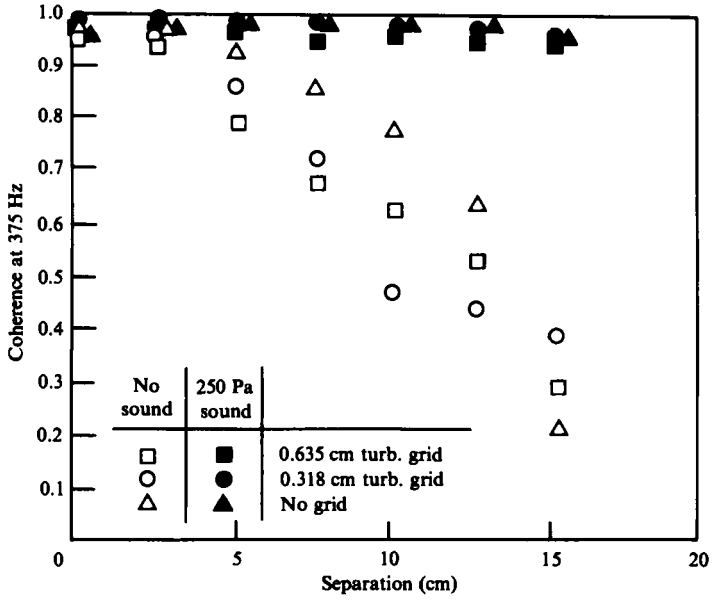

FIGURE 12. Coherence at vortex-shedding peak as a function of separation between flush-film 5 and movable probe with and without sound. Centreline mean velocity is 35 m/s.

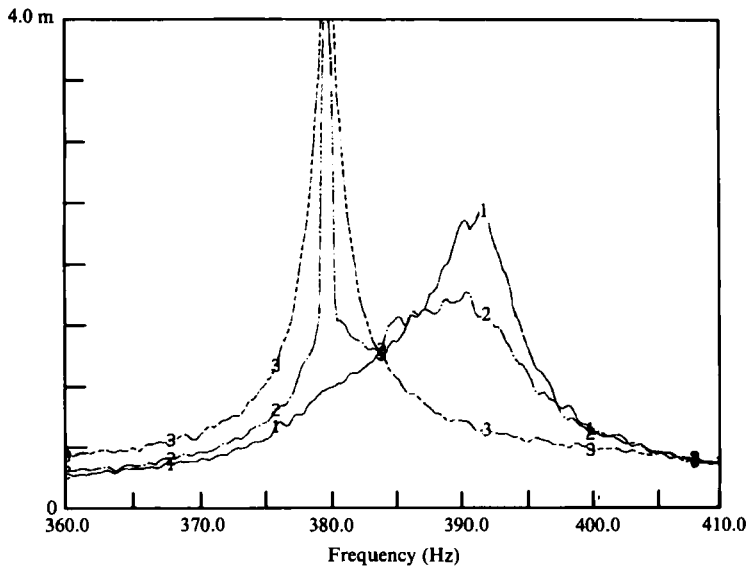

FIGURE 13. Entrainment of vortex shedding at 392 Hz by sound at 380 Hz. Sensor is flush-film 5. This spectrum is the result of 400 consecutively averaged spectra. 1. —, no sound; 2. — · —, 100 Pa sound; 3. – – – –, 250 Pa sound. Note the suppression of the natural vortex-shedding peak at 392 Hz by 250 Pa sound. The vertical scale is not changed for the three different curves.

figure was obtained using signals from two anemometer films: (i) flush-film 5, which is located at mid-height on the test cylinder, and (ii) the movable probe, which was positioned 2.5 cm downstream of the film gauge and could be moved vertically, parallel to the cylinder axis. The dimensionless correlation in figure 12 is defined as the peak in the coherence function, a frequency-domain measure of correlation, at 375 Hz. The 375 Hz value is both the frequency of the applied sound and the peak in the vortex-shedding spectra for these data when averaged over 40 individual consecutive spectra. With sound at 250 Pa, a very high degree of spanwise correlation is obtained. Without sound, correlation drops off sharply after about a 12 diameter separation. These trends are in agreement with the time-history data of figures 7 and 10, and they are not altered by the introduction of turbulence into the free stream.

A series of experiments was performed to determine the effect of sound at frequencies shifted from the centre of the natural vortex-shedding frequency. For these experiments, the sound frequency was held fixed at the resonant frequency of the first transverse acoustic mode of the test section and the mean velocity in the wind tunnel was raised or lowered to shift the vortex-shedding frequency (1). A typical result is shown in figure 13, which shows 400 average spectra at four sound levels from flush-film 5. When no sound is applied, the 35.7 m/s centreline velocity produces a broad vortex-shedding peak at 393 Hz. Application of sound at 100 Pa and 380 Hz reduces the broad vortex peak at 393 Hz and has opened a sharp side lobe at 380 Hz. When the sound amplitude is increased to 250 Pa, the vortex peak entirely disappears but the 380 Hz peak broadens and increases in amplitude. Thus, the sound has shifted the vortex shedding to the applied sound frequency.

Figure 14 shows the ability of sound to shift vortex-shedding frequency. The degree to which sound influences the vortex shedding is a function of the amplitude of the sound and the degree of the frequency shift. As figure 14 (*a*, *b*) shows, when the sound frequency is well removed from the natural vortex-shedding frequency, sound has

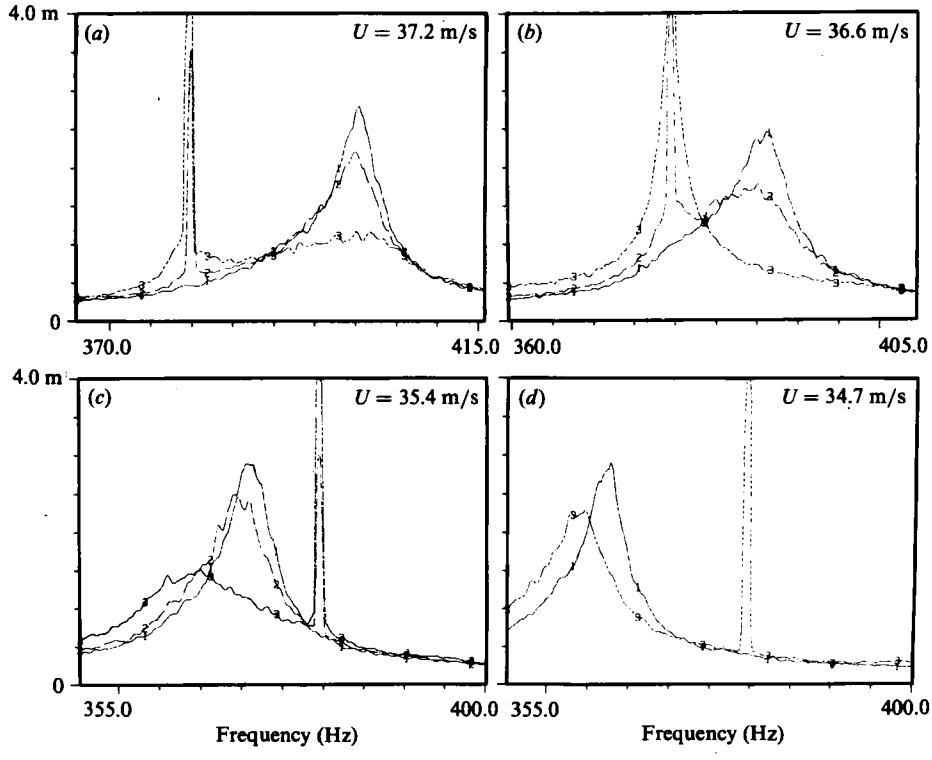

FIGURE 14. Entrainment of vortex shedding by sound at 380 Hz at several mean flow velocities. Sensor is flush-film 5. These spectra are the result of 400 continuously averaged spectra. 1. —, no sound; 2. —·—, 100 Pa sound; 3. – – – –, 250 Pa sound. The vertical scales are not altered for the various sound levels.

relatively little effect on the vortex shedding, and the resultant spectra show just the superposition of the broader vortex-shedding peak and the narrow acoustically induced peak. This is in general agreement with results of Peterka & Richardson (1969), who found that sound imposed at frequencies well above the vortex-shedding frequency had little effect on the shedding frequency. However, when the sound amplitude is sufficiently large and the acoustic frequency is sufficiently close to the natural vortex-shedding frequency, the natural vortex-shedding peak is suppressed and the peak at the acoustic frequency increases (see figures 13 and 14), indicating that the sound has entrained the vortex shedding. Sound applied at frequencies near the vortex-shedding frequency can not only shift the frequency of vortex shedding to the acoustic frequency but can also correlate the vortex shedding along the span of the tube (figure 12) and concentrate the vortex energy at a single frequency. The greatest frequency shift obtained in these tests was about 8% at 300 Pa (150 db) of applied sound. Greater shifts could be obtained to frequencies below the vortex-shedding frequency than to frequencies above it. This may be related to the tendency of the natural vortex-shedding peak to retreat to lower frequencies as sound level is increased (see figure 14*d*).

The shifts in the vortex-shedding frequency of figures 13 and 14 were made with the experimental cylinder in the centre of the test section. Theoretically, the pressure is zero at the centre of the test section in the first acoustic mode (figure 8). This suggests that the acoustic-wave velocity, which is maximum at the centre of the test

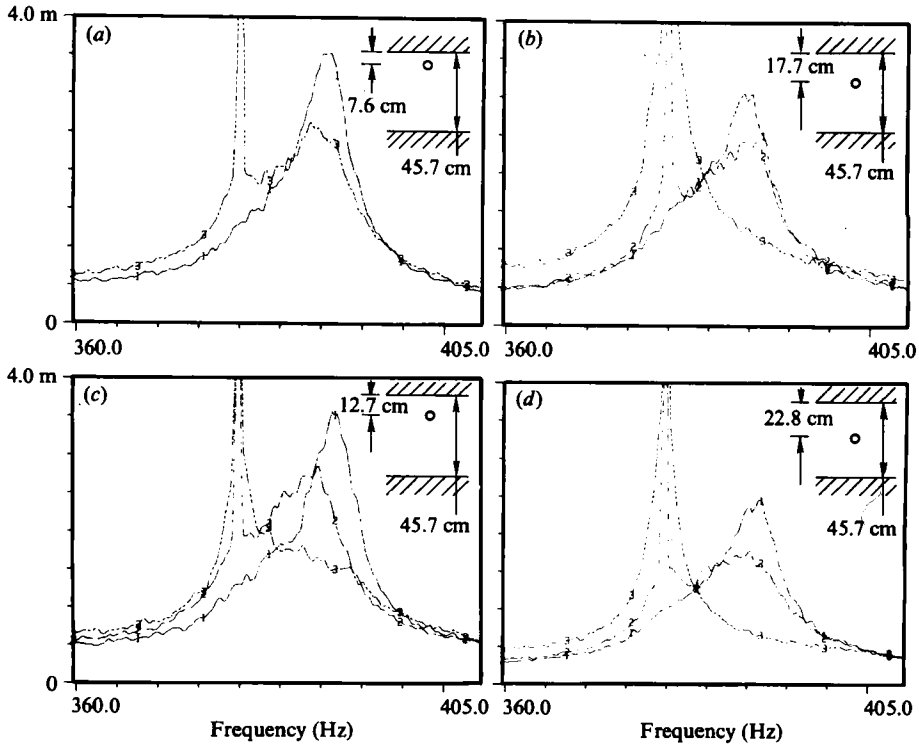

FIGURE 15. Spectra showing increase in entrainment by sound at 380 Hz as cylinder is moved towards centre of test section. $U = 36.6$ m/s. Sensor is flush-film 5. These spectra are the result of 400 consecutively averaged spectra. 1. —, no sound; 2. —·—, 100 Pa sound; 3. – – – –, 250 Pa sound.

section (figure 8; (4)), rather than acoustic pressure was responsible for the entrainment. This hypothesis was tested by moving the test cylinder laterally from its central position towards the test-section wall.

Typical results are shown in figure 15. In each frame in this figure, the transverse location of the test cylinder is shifted by 5.08 cm from its previous position. The centreline velocity is constant at 36.6 m/s in all four frames, which corresponds to a natural vortex-shedding frequency of 385 Hz. Sound is applied at 380 Hz. With the cylinder adjacent to the test-section wall (figure 15*a*), there is relatively little entrainment of vortex shedding by sound even at 250 Pa sound level. The entrainment increases as the cylinder is moved to the centre of the test section (figure 15*d*) when 250 Pa sound completely suppresses the natural vortex-shedding peak at 385 Hz. Since this effectiveness of entrainment follows the predicted acoustic velocity (figure 8), it is reasonable to believe that the entrainment is produced by the acoustic velocity and not the acoustic pressure.

Entrainment was also observed from single tubes with the turbulence grids installed. Figure 16 shows entrainment with the 0.3175 cm and 0.635 cm rod grids installed. Note that, in the absence of sound, the vortex peak becomes increasingly broad as the turbulence level increases and that the ability of sound to entrain the vortex shedding decreases with increasing turbulence levels (compare with figure 9). Since the velocity associated with the turbulence is comparable to the acoustic

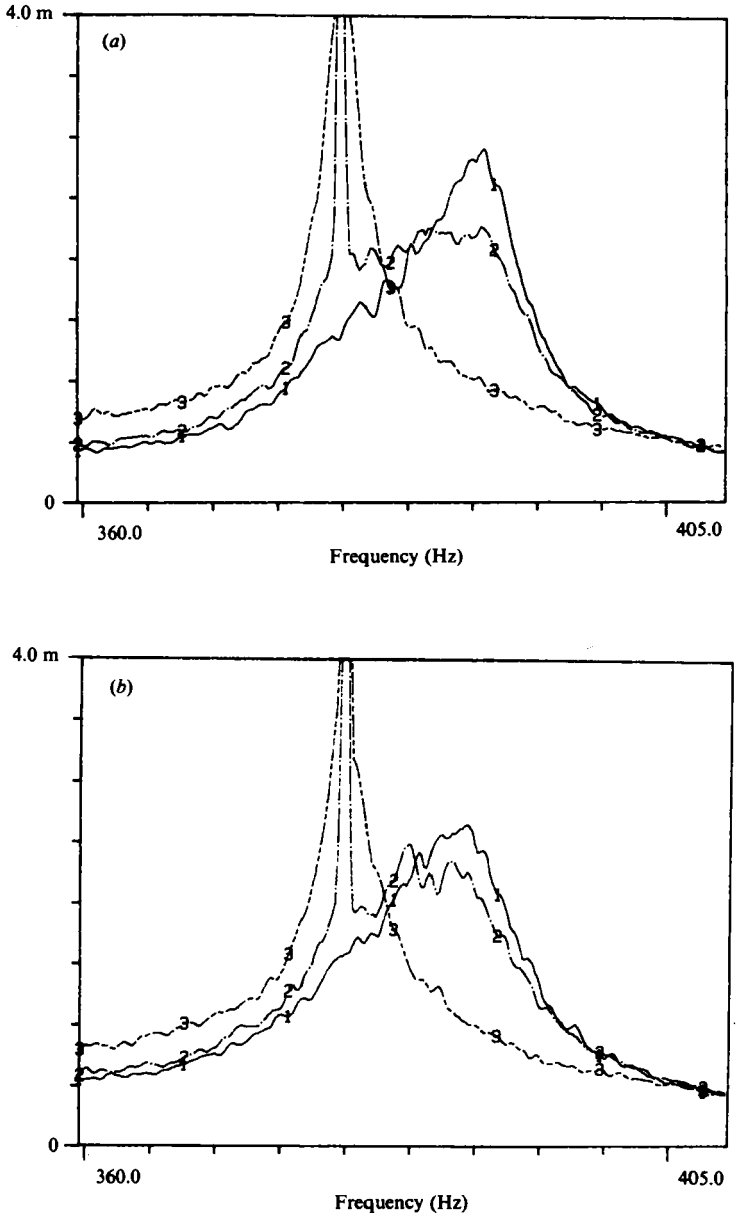

FIGURE 16. Entrainment of vortex shedding by sound at 380 Hz with turbulence grid installed: (*a*) small turbulence grid with 0.318 cm ($\frac{1}{8}$ in.) rods; (*b*) large turbulence grid with 0.635 cm ($\frac{1}{4}$ in.) rods. Sensor is flush-film 5. $U = 36.6$ m/s. These spectra are the result of 400 consecutively averaged spectra. 1. —, no sound; 2. —·—, 100 Pa sound; 3. – – – –, 250 Pa sound.

velocity in figure 16, it is reasonable to believe that sound-induced entrainment can occur only if the acoustic velocity is above the background turbulence velocities.

Entrainment was also observed with a row of four tubes and nine tubes spanning the test section. It therefore appears that acoustic entrainment of vortex shedding also occurs in tube banks of heat exchangers.

5. Discussion

The ability of sound to influence the fluid mechanics of vortex shedding may be tied to the magnitude of the applied (i.e. coherent) sound velocity relative to the background turbulence. A figure of merit θ could be introduced:

$$\theta = \frac{v_{\text{acoustic}}}{u'}. \tag{5}$$

Using (4), for the first-mode excitation, this equation can be expressed in terms of acoustic pressure,

$$\theta = \frac{P\pi \sin(\pi y/L)}{\rho\omega L u'}, \tag{6}$$

which shows how θ decreases at the edges of the test section ($y = 0, L$). This is in agreement with the data shown in figure 15. When θ exceeds 1 and the frequency of the sound is at or near the vortex-shedding frequency, the present data suggests that the sound can entrain the vortex shedding.

This figure of merit could also be applied to a coherent perturbation introduced by cylinder vibration in sympathy with vortex shedding. If the cylinder vibrates at the vortex-shedding frequency (1) at amplitude A, then the amplitude of its surface velocity is $v = 2\pi SUA/D$ and θ becomes

$$\theta = 2\pi S \frac{A}{D} \frac{U}{u_{\text{turbulence}}}.$$

Since $2\pi S \approx 1.25$, this suggests that the relative amplitude (A/D) of vibration must exceed the relative turbulence level in order for the cylinder vibration to influence vortex shedding. This is in general agreement with experimental results. Typically vibration amplitudes on the order of 0.02 to 0.1 diameter are reported in the literature to begin to affect vortex shedding (Sarpkaya 1979).

There are a number of similarities between the effects of applied acoustic field and applied cylinder vibration on vortex shedding from cylinders. In both cases the oscillation must be applied at frequencies near the shedding frequency in order to produce a shift in the shedding frequency. In both cases the spanwise correlation is increased and the apparent transverse momentum of the near wake is increased.

In the present study, 250 Pa sound with velocity, representing about 1.8 % of the free-stream velocity, produced nearly perfect spanwise correlation when applied at the vortex-shedding frequency (figure 12). Toebes (1969) found that a cylinder-vibration amplitude of $A/D = 0.125$, corresponding to a surface velocity of about 15 % of the free-stream velocity, was required to achieve a high degree of spanwise correlation. Koopman (1967) found that a cylinder-vibration amplitude of $A/D = 0.05$ could shift the vortex-shedding frequency by ± 8 %. In the present study, 250 Pa sound produced about the same shift. Koopman (1967) also found the maximum shift increased as the amplitude of vibration increased.

In the absence of sound, the nominal vortex-shedding frequency is given by (1). With sound, the preferred vortex-shedding frequency may shift. Figures 13 and 14 show that the ability of sound to suppress vortex-shedding frequency at the natural frequency (1) and shift it to the applied frequency is greater when the sound is applied at frequencies below the shedding frequency. The tendency for the phase angle between sound and vortex shedding to decrease with increasing sound (figure 11) is also indicative of a downward shift in the preferred vortex-shedding frequency as sound is applied. Thus, if the vortex shedding is modelled as an oscillator, it would

be of a softening type. That is, the natural frequency of the oscillator should decrease as its amplitude increases. One result of this softening effect could be a hysteretic effect as forcing is swept up or down through the shedding frequency. A hysteretic effect was not observed in these tests, but hysteresis has been observed with vortex shedding from vibrating cylinders (Bishop & Hassan 1964).

Typical measurements of spanwise correlation of vortex shedding, in the absence of external excitation, range from 3 to 15 diameters in the Reynolds-number range between 1000 and 100000 (Sarpkaya 1979). It is reasonable to believe that these spanwise cell vortices, like all vortices, induce velocity fields on one another that then influence their dynamics. Moreover, small differences in mean velocity at different spanwise locations, velocity changes in time, the unsteady behaviour associated with boundary-layer transition over the cylinders, or simply vortex-induced velocity components produce the potential for different preferred natural frequencies of vortices along the span. However, because the vortices induce velocity fields on one another, the result is not multiple tones but rather a single tone that wanders in frequency. This phenomenon could be modelled by multiple, coupled self-excited oscillators.

The ability of sound to shift the frequency of vortex shedding could explain the persistence of acoustic resonances in heat exchangers. At low flow rates, the frequency of vortex shedding from the heat-exchanger tubes will be well below the acoustic natural frequencies of the gas contained within the heat-exchanger shell. The aeroacoustic sound of the vortex shedding will not be amplified, and so feedback of this sound into vortex shedding will be minimal. As flow is raised, so that the shedding from some portion of some of the tubes coincides with the fundamental acoustic frequency, then this portion of the sound spectrum will be amplified.

If sound levels above about 60 Pa (130 db) result, the amplified sound will tend to synchronize the vortex shedding and increase the coherence of vortex shedding. This leads to higher sound levels that will in turn synchronize shedding from tubes which are exposed to perhaps slightly different mean gas velocities. The resultant sound level will be limited by the acoustic dissipation, the distribution of flow, and the maximum strength of the shed vortices. Once a high level of sound is established, it will tend to persist at the same frequency even as the mean gas velocity is varied because the acoustic natural frequency at which sound is amplified remains constant. Large increases in velocity will eventually break the synchronization until the next-higher acoustic mode becomes excited.

6. Conclusions

The conclusions of this study of the effect of transverse standing sound waves on vortex shedding from cylinders in crossflow in a duct are as follows:

(i) In the absence of sound, vortex shedding is not a steady harmonic process when examined at high resolution. Rather it is a series of coherent strings of events whose frequencies wander 1–2% about the nominal vortex-shedding frequency. Very irregular high-frequency cycles interspace the larger-amplitude coherent strings, which are nearly sinusoidal.

(ii) When sound greater than about 60 Pa (130 db) (measured at the test-section walls) is applied at the frequency of vortex shedding, the frequency wander is eliminated. The vortex shedding correlates with the sound, the amplitude increases, and the shedding becomes well correlated along the cylinder span.

(iii) Sound applied at frequencies near the natural vortex-shedding frequency can

shift vortex shedding to the sound frequency. The greater the sound amplitude, the greater the frequency shift that could be achieved. Shifts of 8 % with 300 Pa (144 db) sound were achieved in these tests. It is likely that, with larger-amplitude sound, greater shifts could be achieved.

(iv) There is a tendency for the preferred vortex-shedding frequency to decrease when sound is applied. Thus, for example, greater shifts could be achieved when sound is applied below the vortex-shedding frequency than above it.

(v) Sound has the greatest influence on vortex shedding with the cylinder located at a node (i.e. minimum) of sound pressure. This suggests that it is not sound pressure but rather the velocity induced by sound which influences vortex shedding.

(vi) Turbulence in the free stream tends to suppress the influence of sound. The data suggest that the sound-induced velocity must exceed the turbulence velocities in order for sound to influence vortex shedding.

(vii) The ability of sound to influence vortex shedding observed from single tubes also occurs in rows of tubes across the test section. Probably similar phenomena occur in arrays of tubes. The feedbacks between self-sound and vortex shedding could create a persistent and intense acoustic resonance.

The author is indebted to M. W. Bressler and R. Dexter, who performed these experiments, to G. Schnitz and J. P. Smith, who built the experimental apparatus, to Dr K. N. Helland and Dr J. C. LaRue, who consulted on the wind-tunnel design and anemometry, and to Dr J. M. Greene for theoretical discussions. The author would like to thank Dr Oscar P. Manley for his support and encouragement. This work was supported by the U.S. Department of Energy, Office of Basic Energy Sciences, under Contract DE-AT03-82ER12023.

REFERENCES

Baird, R. C. 1954 Pulsation-induced vibration in utility steam generation units. *Combustion* **25** (10), 38–44.

Baylac, G. & Gregoire, J. P. 1975 Acoustic phenomena in a steam generating unit. *J. Sound Vib.* **42**, 31–48.

Bishop, R. E. D. & Hassan, A. Y. 1964 The lift and drag forces on a circular cylinder in flowing field. *Proc. R. Soc. Lond.* A **277**, 51–75.

Blevins, R. D. 1977 *Flow-Induced Vibration*. Van Nostrand Reinhold.

Blevins, R. D. 1984 Review of sound induced by vortex shedding from cylinders. *J. Sound Vib.* **92**, 455–470.

Donaldson, I. S. & McKnight, W. 1979 Turbulence and acoustic signals in a cross-flow heat exchanger model. In *Flow-Induced Vibrations*, pp. 123–128. American Society of Mechanical Engineers.

Grotz, B. J. & Arnold, F. R. 1956 Flow-induced vibrations in heat exchangers. *Tech. Rep. No.* 31, *DTIC No.* 104568. Department of Mechanical Engineering, Stanford University.

Itsweire, E. C. & Hell, K. N. 1983 A high-performance low-cost constant-temperature hot wire anemometer. *J. Phys.* E: *Sci. Instrum.* **16**, 549–553.

King, R. 1977 A review of vortex-shedding research and its application. *Ocean Engng* **4**, 141–171.

Koopman, G. H. 1967 Vortex wakes of vibrating cylinders at low Reynolds numbers. *J. Fluid Mech.* **28**, 501–512.

Morse, P. M. & Ingard, K. U. 1968 *Theoretical Acoustics*. McGraw-Hill.

Okamoto, S., Hirose, T. & Adachi, T. 1981 The effect of sound on the vortex shedding from a circular cylinder. *Bull. Japan. Soc. Mech. Engrs* **24**, 45–53.

PETERKA, J. A. & RICHARDSON, P. D. 1969 Effects of sound on separated flows. *J. Fluid Mech.* **37**, 265–287.

PUTNAM, A. A. 1965 Flow-induced noise in heat exchangers. *J. Engng Power* **81**, 417–422.

RICHARDSON, P. D. 1967 Effects of sound and vibration on heat transfer. *Appl. Mech. Rev.* **20**, 201–217.

ROSHKO, A. 1953 On the development of turbulent wakes from vortex streets. *NACA-TN*-2913.

SARPKAYA, T. 1979 Vortex-induced oscillations; a selective review. *J. Appl. Mech.* **46**, 241–258.

TOEBES, G. H. 1969 The unsteady flow and wake near an oscillating cylinder. *Trans. ASME* D: *J. Basic Engng* **91**, 493–498.